ISSN 0006-2979, Biochemistry (Moscow), 2024, Vol. 89, No. 10, pp. 1744-1758 © Pleiades Publishing, Ltd., 2024.

Glioblastoma Sensitization to Therapeutic Effects by Glutamine Deprivation Depends on Cellular Phenotype and Metabolism

Alina A. Isakova[1,2], Irina N. Druzhkova[3], Artem M. Mozherov[3], Diana V. Mazur[1], Nadezhda V. Antipova[1], Kirill S. Krasnov[4], Roman S. Fadeev[4], Marine E. Gasparian[1], and Anne V. Yagolovich[2,a]*

[1]*Shemyakin–Ovchinnikov Institute of Bioorganic Chemistry, Russian Academy of Sciences, 117997 Moscow, Russia*

[2]*Lomonosov Moscow State University, 119991 Moscow, Russia*

[3]*Privolzhsky Research Medical University, 603081 Nizhny Novgorod, Russia*

[4]*Institute of Theoretical and Experimental Biophysics, Russian Academy of Sciences, 142290 Pushchino, Moscow Region, Russia*

[a]*e-mail: anneyagolovich@gmail.com*

Received June 3, 2024
Revised August 23, 2024
Accepted September 5, 2024

Abstract—Glutamine plays an important role in tumor metabolism. It is known that the core region of solid tumors is deprived of glutamine, which affects tumor growth and spread. Here we investigated the effect of glutamine deprivation on cellular metabolism and sensitivity of human glioblastoma cells U87MG and T98G to drugs of various origin: alkylating cytostatic agent temozolomide; cytokine TRAIL DR5-B – agonist of the DR5 receptor; and GMX1778 – a targeted inhibitor of the enzyme nicotinamide phosphoribosyltransferase (NAMPT), limiting NAD biosynthesis. Bioinformatics analysis of the cell transcriptomes showed that U87MG cells have a more differentiated phenotype than T98G, and also differ in the expression profile of the genes associated with glutamine metabolism. Upon glutamine deprivation, growth rate of the U87MG and T98G cells decreased. Analysis of cellular metabolism by FLIM microscopy of NADH as well as assessment of lactate content in the medium showed that glutamine deprivation shifted metabolic status of the U87MG cells towards glycolysis. This was accompanied by the increase in expression of the stemness marker CD133, which collectively could indicate de-differentiation of these cells. At the same time, we observed increase in both expression of the DR5 receptor and sensitivity of the U87MG cells to DR5-B. On the contrary, glutamine deprivation of T98G cells induced metabolic shift towards oxidative phosphorylation, decrease in the DR5 expression and resistance to DR5-B. The effects of NAMPT inhibition also differed between the two cell lines and were opposite to the effects of DR5-B: upon glutamine deprivation, U87MG cells acquired resistance, while T98G cells were sensitized to GMX1778. Thus, phenotypic and metabolic differences between the two human glioblastoma cell lines caused divergent metabolic changes and contrasting responses to different targeted drugs during glutamine deprivation. These data should be considered when developing treatment strategies for glioblastoma via drug-mediated deprivation of amino acids, as well as when exploring novel therapeutic targets.

DOI: 10.1134/S0006297924100079

Keywords: glutamine deprivation, glioblastoma, cell differentiation, CD133, TRAIL, DR5, NAD(P)H, FLIM microscopy, NAMPT, GMX1778

Abbreviations: CD133, prominin-1; DR5, death receptor 5; FLIM, fluorescence-lifetime imaging microscopy; NADH, reduced form of nicotinamide adenine dinucleotide; NAMPT, nicotinamide phosphoribosyltransferase; OXPHOS, oxidative phosphorylation; TRAIL, Tumor necrosis factor-related apoptosis-inducing ligand.

* To whom correspondence should be addressed.

INTRODUCTION

Tumor cells are characterized by intense metabolic processes that require increased consumption of nutrients. Glutamine is one the most abundant non-essential amino acids in the body [1]. High glutamine consumption by tumor cells is an adaptive metabolic mechanism that promotes proliferation under conditions of hypoxia and nutrient deficiency. During glutaminolysis, glutamine is converted into glutamate and α-ketoglutarate. Glutamine is a carbon and nitrogen donor for the synthesis of reduced glutathione (GSH), thereby regulating redox status of tumor cells [2]. Glutamine has been shown to be an anaplerotic precursor for tricarboxylic acid cycle; in addition, the product of glutaminolysis is NAD(P)H, which ensures other anabolic processes [3]. Lack of glutamine can affect tumor growth: for example, glutamine deprivation in osteosarcoma cells caused increase in secretion of the pro-inflammatory chemokine interleukin-8 (IL-8) [4]; also, glutamine deficiency promoted c-MYC-mediated apoptosis [5]. Glutamine metabolism can be reprogrammed by the oncogenes c-MYC, KRAS, PI3K/AKT/mTOR, and tumor suppressor p53 [2].

In solid tumors, there is spatial heterogeneity in distribution of oxygen and nutrients, which results in local hypoxia. Similarly, there is local deficiency of glutamine in tumors, which could be one of the factors of resistance to chemotherapy [6]. Among the solid tumors, glioblastoma is particularly dependent on glutamine metabolism, since homeostasis of the neurotransmitter glutamate, which originates from glutamine, is required for normal brain function. In glioblastoma, local glutamine deprivation was also shown, which was more pronounced deep in the tumor [7, 8]. Drug therapy for glioblastoma is currently limited primarily to temozolomide, an alkylating-type cytostatic chemotherapy drug. However, given its insufficient efficacy, a search for new promising molecular targets is necessary [9]. The death receptor DR5 is known to be a prognostic marker for the patients with glioblastoma [10], and use of the DR5 agonists in the treatment of glioblastoma has also been investigated [11]. Another promising target is NAMPT, an enzyme that catalyzes synthesis of nicotinamide mononucleotide, which is the rate-limiting step in NAD biosynthesis. NAMPT inhibitors have potential for treatment of solid tumors, including glioblastoma [12].

A number of strategies for drug-induced glutamine deprivation in combination with other anticancer drugs are being developed to enhance therapeutic efficacy [13, 14]. The work aimed at investigating the effect of glutamine deprivation on metabolism of the human glioblastoma cells and their sensitivity to therapeutic effects of the drugs of different nature: conventional chemotherapeutic drug temozolomide [15], DR5 receptor agonist – modified cytokine TRAIL DR5-B [16], as well as small molecule targeted inhibitor of NAMPT – GMX1778 [17].

MATERIALS AND METHODS

Cell culturing. U87MG and T98G glioblastoma cell lines were obtained from the ATCC (USA) and cultured in a DMEM nutrient medium (PanEco, Russia, Cat. No. C420p) containing 4.5 g/l glucose and 110 mg/ml sodium pyruvate, with addition of 10% fetal calf serum (HyClone, USA, Cat. No. K052/SV30 160.03), 2 mM L-glutamine (PanEco, Russia, Cat. No. F032), penicillin (100 μg/ml) and streptomycin (100 μg/ml) (PanEco, Russia, Cat. No. A073p) at 37°C and 5% CO_2. To simulate glutamine deprivation, cells were incubated in a L-glutamine-free medium for at least 72 h.

Transcriptome sequencing. RNA sequencing was performed at Genoanalitika, on a HiSeq1500 device (Illumina, USA) generating at least 40 million short reads with length of 150 nucleotides. Using the STAR software (version 2.7.9a), the initial reads were mapped to the GRCh38 genome, and number of the reads mapped to individual genes (Ensembl annotation, version 99) with no more than three mismatches was counted. RNA sequencing for each group was performed in duplicate.

Differential gene expression analysis. Differential gene expression in the U87MG cell culture relative to T98G was evaluated using the DEseq2 package version 1.28.1 [18] for the R programming language version 4.2.2. Gene Sets Enrichment Analysis (GSEA) was performed using the Molecular Signature DataBase MsigDB [19] and the GSEApy library for the Python programming language version 3.11.7 version 1.0.6 [20]. For analysis, we used a ranked list of genes sorted by decreasing fold change in expression, obtained by calculating differential gene expression (GSEA preranked). To study in detail changes in the cell transcriptional activity, GSEA was performed using gene sets from the curated GeneOntology databases (subcollections GO: Biological Processes GO:BP, GO: Cellular Components GO:CC, and GO: Molecular Functions GO:MF) [21], Kyoto Encyclopedia of Genes and Genomes (KEGG) [22], Reactome [23], WikiPathways (WP) [24], Protein Interaction Database (PID) [25], Transcription Factor Targets Legacy (TFT Legacy) [26]. To assess changes in the transcriptional activity of the genes associated with glutamine metabolism, a list of genes was obtained from the Reactome Glutamate and Glutamine Metabolism database gene set, for which fold change in expression (logFC) values were used. To assess significance of gene expression changes using DESeq2, the Wald test with correction for Benjamini–Hochberg multiple testing (FDR) was used [27]. All data are presented for FDR ≤ 0.05.

Table 1. Primers for RT-qPCR

No.	Name	Sequence (5′->3′)	
		Forward	Reverse
1	$p21^{Waf1}$ (CDKN1A-F110)	AGTCAGTTCCTTGTGGAGCC	CATTAGCGCATCACAGTCGC
2	$p27^{KIP1}$ (CDKN1B-F115)	TGTTTCAGACGGTTCCCCAAA	CCATTCCATGAAGTCAGCGAT
3	CD133	ACTCCCATAAAGCTGGACCC	TCAATTTTGGATTCATATGCCTT
4	DR5	TGGAACAACGGGGACAGAACG	GCAGCGCAAGCAGAAAAGGAG
5	cFLIP	GGCTCCCCCTGCATCACATC	CCGCAGTACACAGGCTCCAGA
6	18S	GGCCCTGTAATTGGAATGAGTC	CCAAGATCCAACTACGAGCTT

Quantitative reverse transcription PCR (RT-qPCR). Total RNA was isolated using an ExtractRNA reagent (Evrogen, Russia). RNA concentration was determined using a Nanodrop One C spectrophotometer (Thermo Fisher Scientific, USA). Total RNA was used as a template for cDNA synthesis using a MMLV RT kit (Evrogen) according to the manufacturer's instructions. Amplification was carried out for 5 min at 10°C, and then for 25 min at 37°C and 42°C, respectively, and at 70°C for 10 min to inactivate the enzyme. Real-time PCR was performed with a LightCycler 96 (Roche) using a qPCRmix-HS SYBR reagent (Evrogen) according to the manufacturer's instructions according to the following program: 95°C for 150 s, 45 cycles of 95°C for 20 s, 60°C for 20 s and 72°C for 20 s. Data acquisition was performed using the LightCycler Software (version 4.1). Absence of PCR byproducts was determined from melting curves. For each primer pair, identical PCR melting peaks of each sample were observed in triplicate across all samples. The obtained Ct (cycle threshold) values for each sample did not exceed 35. Ribosomal 18S RNA gene was used as an internal control. Relative gene expression levels were calculated with the $2^{-\Delta\Delta CT}$ method. Visualization and statistical data processing were performed using the GraphPad Prism 9.3.1 (GraphPad Software, USA). Cell samples were compared with each other using one-way ANOVA. Differences were considered significant at $p < 0.05$. Primers for detecting expression of the $p21^{Waf1}$, $p27^{KIP1}$, CD133 (prominin-1), DR5, and cFLIP genes are listed in Table 1.

Fluorescent-lifetime imaging microscopy (FLIM). FLIM of the metabolic cofactor NADH (reduced form of nicotinamide adenine dinucleotide) was performed using a laser scanning microscope LSM 880 (Carl Zeiss, Germany). A femtosecond Ti:Sa laser (Spectra Physics, USA) with a pulse repetition rate of 80 MHz and duration of 120 fs was used as an excitation source. Detection of fluorescence lifetimes was performed using a TCSPC FLIM module (Becker & Hickl GmbH, Germany), based on time-correlated single-photon counting. To obtain images, a 40×/1.3 oil immersion objective was used. NAD(P)H fluorescence was excited in a two-photon mode at a wavelength of 750 nm, and the signal was recorded in the range of 450-490 nm. Power of the exciting radiation was 7 mW. Photon acquisition time was 60 s. Number of photons per pixel was no less than 5000. During the experiment, the cells were in an incubator at 37°C, 5% CO_2. FLIM data were processed using the SPCImage software (Becker & Hickl GmbH). Least squares approximation was used to obtain parameters of the decay curves at each pixel. NAD(P)H fluorescence decay curves were fitted by a bi-exponential model. Approximation accuracy was assessed using the $\chi 2$ parameter. For all data, $\chi 2$ ranged from 0.8 to 1.2. Short and long decay components ($\tau 1$ and $\tau 2$, respectively), relative amplitudes of these components ($\alpha 1$ and $\alpha 2$), as well as average fluorescence lifetime ($\tau m = \alpha 1\tau 1 + \alpha 2\tau 2$) were estimated. Autofluorescence analysis was performed for each cell individually in the cytoplasmic region. For each group, at least 5 images were obtained with a total number of cells of at least 30.

Assessment of cell glycolytic activity from lactate content in the culture medium. U87MG and T98G cells were seeded in a 6-well plate at 5×10^5 cells per well and cultured in a medium with or without glutamine for 20 h. Then the culture medium was collected and proteins were removed using a deproteinization kit (ab204708, Abcam, USA). Samples were analyzed using a colorimetric lactate assay kit (MAK064, Sigma-Aldrich, USA). Amount of lactate was assessed from optical density of the solution at a wavelength of 570 nm using a SYNERGYmx microplate reader (BioTek, USA).

Flow cytometry. To analyze surface expression of DR5 receptor, U87MG and T98G cells were seeded in 6-well plates at 2×10^5 cells per well and cultured at 37°C, 5% CO_2 with or without glutamine for at least 72 h. Cells were detached with a Versene solution, washed

with an ice-cold PBS, resuspended in a FACS buffer (1% BSA in PBS), and incubated for 1 h at 4°C with 5 μg/ml of monoclonal antibodies against DR5 (clone DR5-01-1, GeneTex, USA). Cells were then washed twice and incubated for 1 h at 4°C with 20 μg/ml of a secondary antibody Dylight 488 (GeneTex), washed, and resuspended in FACS buffer containing propidium iodide. DR5 receptor expression was determined using a CytoFlex flow cytometer (Beckman Coulter, USA) using mouse IgG1 as an isotype control.

Production of a recombinant DR5-specific TRAIL variant DR5-B. Recombinant DR5-B protein was expressed in *E. coli* SHuffle B cells and purified from the soluble cellular fraction by nickel affinity and ion exchange chromatography as described previously [28].

Cytotoxicity assay. U87MG or T98G cells were seeded into 96-well plates at 1×10^4 cells per well. After 24 h, temozolomide (Macklin, China), DR5-B or GMX1778 were added to the cells at the indicated concentrations and incubated for 72 h. Temozolomide and GMX1778 were pre-dissolved in DMSO at concentration of 1 M and 100 mM, respectively, and added to the cells so that final DMSO content in the well did not exceed 0.5% and did not exhibit a cytotoxic effect. Then 0.05% MTT was added to the cells, incubated for 4 h, and the formed crystals were dissolved in DMSO (100 μl per well). Absorbance was measured at 570 nm using an iMark plate spectrophotometer (Bio-Rad, USA).

Statistical analysis. The obtained data were normally distributed and expressed as a mean or a mean ± standard deviation. Normality of the distribution was assessed using the Shapiro–Wilk test. No significant outliers were observed. Statistical analysis of all results except differential gene expression was carried out using Student's *t*-test. The experiments were performed in triplicate. The results were processed using GraphPad Prism 8.0.1 (USA). Differences were considered significant at $p < 0.05$.

RESULTS

Human glioblastoma cells U87MG have more differentiated phenotype compared to T98G. In this work, human glioblastoma cell lines U87MG and T98G were studied. To compare characteristics and differences of the two cell lines, transcriptome sequencing was performed under standard culture conditions. Analysis of differential gene expression between the U87MG and T98G cell lines by functional affiliation of the gene sets (GSEA, Gene Sets Enrichment Analysis) from the GO:BP database showed increased activity of the genes associated with major histocompatibility complex class II in the U87MG cells relative to the T98G cells (Fig. 1a). Similar results were obtained when analyzing the genes from the GO:CC and GO:MF subcollections (Fig. 1b). This suggests that the U87MG cells have a more differentiated phenotype compared to the T98G cells [29, 30]. Analysis using the sets of genes from the KEGG, WP, Reactome, and PID collection (Fig. 2a) showed increased activity of the genes involved in signal transduction processes in the U87MG cells due to generation of the secondary signaling molecules, as well as in the PD-1 signaling pathway, which could be one of the factors of cellular resistance to TRAIL [31]. In addition, the GSEA analysis was performed using transcription factor (TF) target gene sets (TFT-Legacy collection), which could indirectly indicate activity of the genes under control of the specific TFs (Fig. 2b). Transcriptional activity of the genes under control of transcription factors EN, RSRFC4 (MEF2A), EVI1 (MECOM), FOXJ2, CDPCR3 (CUTL1, CUX1), RORA2 (RORA), NKX25 (NKX2-5), PAX4, HFH1 (FOXQ1), and FOXD3 was increased in the U87MG cells relative to the T98G cells. Activity of these transcription factors is important for regulation of cell differentiation, indicating a more differentiated phenotype of the U87MG cells compared to the T98G cells.

U87MG and T98G cells differ in the level of transcriptional activity of the genes associated with glutamine metabolism. Analysis of the changes in the transcriptional activity of the genes associated with glutamine metabolism from the GSEA MSigDB Reactome Glutamate and Glutamine Metabolism databases showed statistically significant increase in the expression of glutamate dehydrogenase 1 (GLUD1), involved in glutamate catabolism [32], but not its paralog GLUD2, in the U87MG cells relative to the T98G cells (Fig. 2c). At the same time, expression of a number of other genes in the U87MG cells was significantly lower than in the T98G cells: mitochondrial aspartate aminotransferase (GOT2), which is associated with reduced glutamine metabolism and cellular senescence [33]; cytoplasmic (PYCR3) and mitochondrial (PYCR1) pyrroline-5-carboxylate reductases, catalyzing biosynthesis of proline from glutamate as a precursor [34]; glutamine synthetase (GLUL), catalyzing endogenous synthesis of glutamine from glutamate [32]; and N-acetyl-aspartyl-glutamate synthase A (NAAGSA, RIMKLA), metabolizing glutamate [35]. There were no significant changes in the expression of other genes involved in glutamine metabolism (Fig. 2c).

Glutamine deprivation reduces growth rate of the U87MG and T98G cells and increases expression of the stem cell marker CD133 and the cyclin-dependent kinase inhibitors $p21^{Waf1}$ and $p27^{KIP1}$ in the U87MG cells. Glutamine-free cell culturing led to the decrease in the growth rate of U87MG and T98G cells to varying degrees (Fig. 3a), which is consistent with the previously published data [36, 37]. Since U87MG and T98G cells differ in their initial differentiation state, we assessed the change in expression

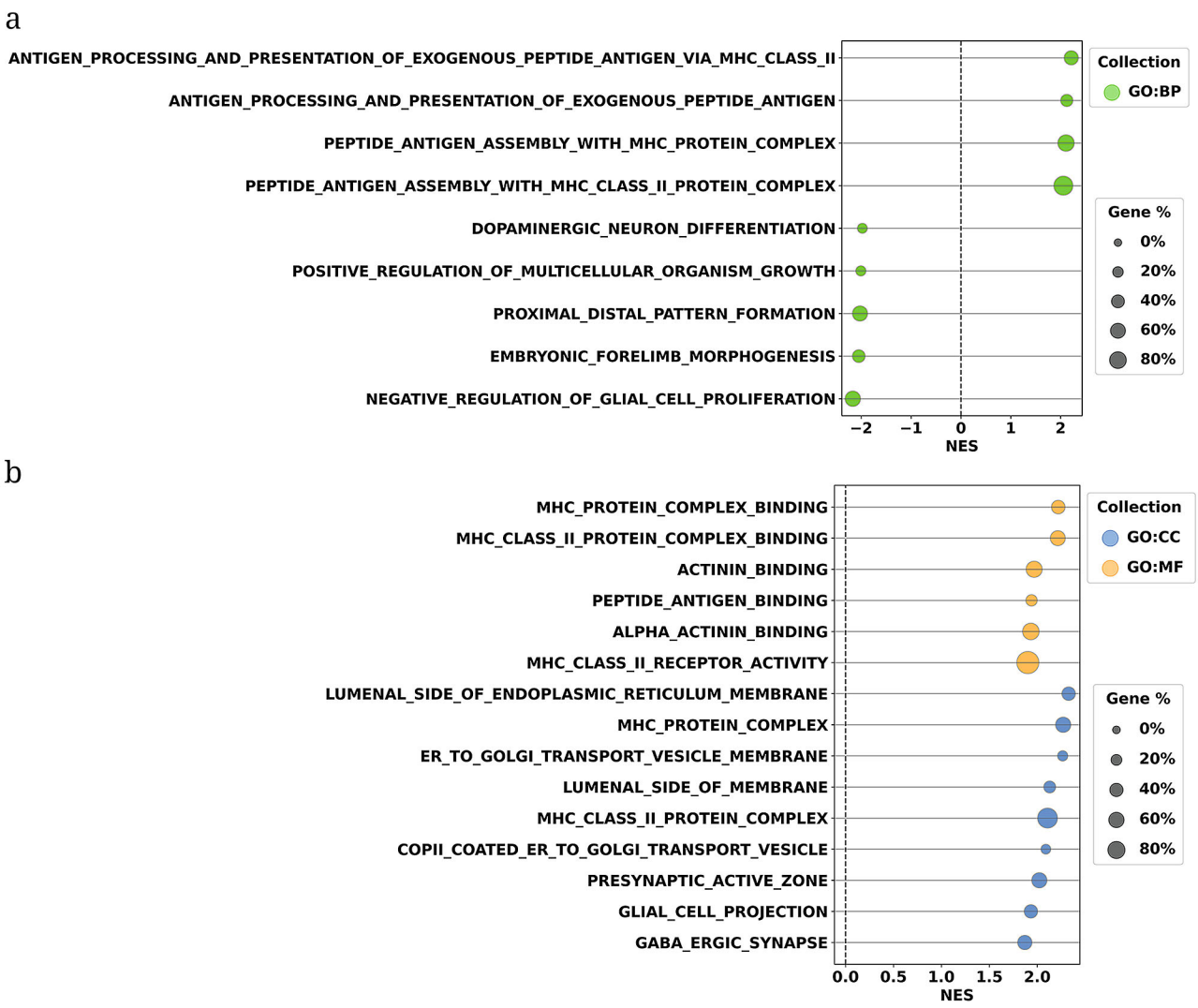

Fig. 1. Comparative analysis of GSEA gene sets in the U87MG cells relative to T98G cells. GSEA results for GO:BP (a), GO:CC and GO:MF (b) collections. Diameter of the circle is proportional to the ratio of the number of differentially expressed genes versus total number of genes in the set. NES, normalized enrichment score. FDR ≤ 0.05.

of the glioma stem cell marker CD133 upon glutamine deprivation using RT-qPCR. The level of CD133 expression increased in the U87MG cells, which could indicate the process of de-differentiation of these cells. In the T98G cells, the CD133 marker was not detectable regardless of the presence of glutamine (Fig. 3b). A similar effect was observed for the expression of inhibitors of cyclin-dependent kinases $p21^{Waf1}$ and $p27^{KIP1}$: significant increase in the expression was observed in the U87MG cells, but not in the T98G cells (Fig. 3c).

Glutamine deprivation induces contrasting metabolic effects in U87MG and T98G cells as revealed by FLIM. Changes in the metabolism of U87MG and T98G cells upon glutamine deprivation were studied using metabolic imaging based on two-photon fluorescence-lifetime imaging microscopy (FLIM) of NADH autofluorescence. The phosphorylated form NADPH, which is characterized by the longest fluorescence lifetime of ~4.4 ns [38], was not detected in the analyzed cell cultures. When cultured with glutamine, percentage contributions of free (α1) and bound NADH forms for the U87MG and T98G cells did not differ initially (Table 2). Analysis of the NADH autofluorescence parameters showed typical lifetime values of the free (τ1) and protein-bound forms (τ2) [39, 40]. Upon glutamine deprivation in the U87MG cells, decrease in the average fluorescence lifetime (τm), lifetime of the free form (τ1), and increase in the contribution of the free form (α1) were observed, which together could indicate shift of the cell metabolism towards glycolysis. At the same time, lifetime of the protein-bound form (τ2) remained unchanged. In the T98G cells, on the contrary, increase in the parameters τm and τ1 was observed, and the glycolysis-associated contribution of the free form α1 significantly decreased, which

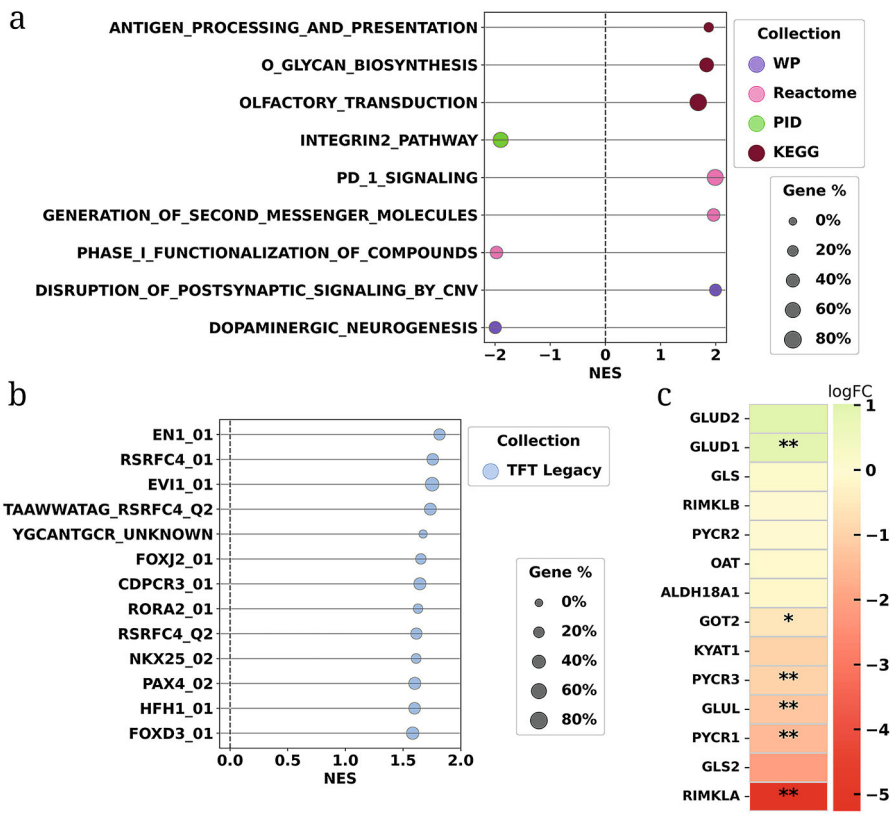

Fig. 2. Comparative analysis of GSEA gene sets in the U87MG cells relative to T98G cells. a) GSEA results for KEGG, PID, Reactome, WP; b) TFT Legacy collections. Diameter of the circle is proportional to the ratio of the number of differentially expressed genes versus total number of genes in the set. NES, normalized enrichment score. FDR ≤ 0.05. c) Fold change (FC) in the expression of genes associated with glutamine metabolism from the Reactome Glutamate and Glutamine Metabolism database in the U87MG cells relative to T98G cells (logFC). * FDR ≤ 0.05; ** FDR ≤ 0.01.

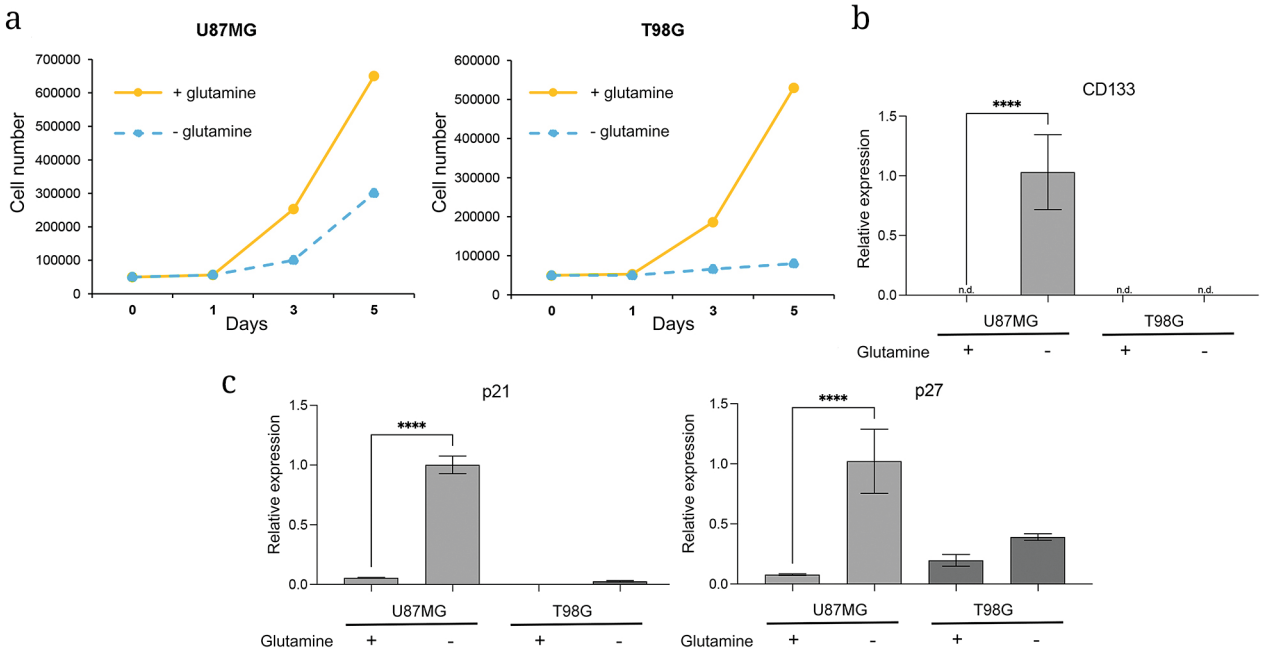

Fig. 3. Effects of glutamine deprivation on U87MG and T98G cell lines. a) Growth rate of U87MG and T98G cells in the absence or presence of glutamine. b) Changes in the expression levels of CD133. c) $p21^{Waf1}$ and $p27^{KIP1}$ at the mRNA level determined by RT-qPCR. **** $p < 0.005$.

Table 2. Parameters of NADH autofluorescence in U87MG and T98G cells in the absence or presence of glutamine (mean ± SD)

Cell line	Glutamine	τm, ns	τ1, ns	τ2, ns	α1, %
U87MG	+	0.84 ± 0.07	0.42 ± 0.03	2.47 ± 0.19	79.31 ± 1.74
	–	0.74 ± 0.07* $p < 0.001$	0.37 ± 0.04 $p < 0.001$	2.32 ± 0.18 $p < 0.001$	81.16 ± 1.60* $p < 0.001$
T98G	+	0.86 ± 0.08	0.46 ± 0.04	2.46 ± 0.21	79.84 ± 1.95
	–	0.99 ± 0.10* $p < 0.001$	0.51 ± 0.05* $p < 0.001$	2.73 ± 0.24 $p < 0.001$	77.56 ± 2.07* $p < 0.001$

Note. τ1 and τ2 are fluorescence lifetimes of the free and protein-bound NADH, respectively, τm is average fluorescence lifetime of NADH, α1 is percentage contribution of the free form of NADH.

* Significant difference from the control, $p < 0.001$.

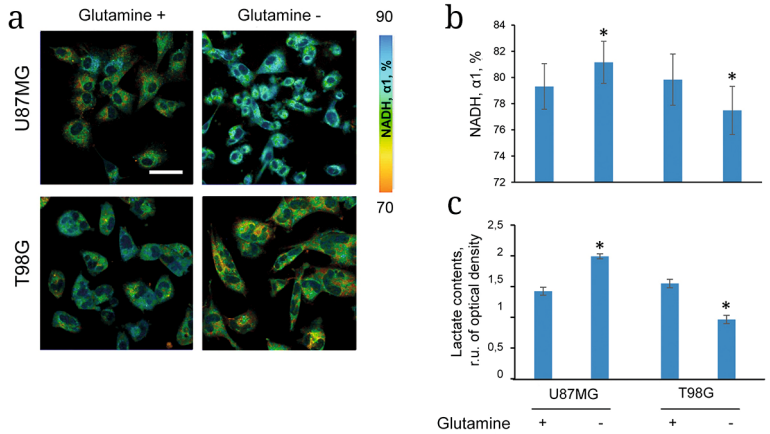

Fig. 4. Study of the metabolic status of U87MG and T98G cells upon glutamine deprivation. a) Microscopic pseudo-colored FLIM images of the free form NADH contribution ratio, α1; scale bar: 50 μm for all images. b) Quantification of NADH, α1, by FLIM. Bar graphs represent a mean ± SEM. * Statistically significant deviation from the "glutamine+" group, $p < 0.005$. c) Evaluation of lactate content in the culture medium by colorimetric method at a wavelength of 570 nm. Bar graphs represent a mean optical density of the solution ± SEM, * $p < 0.001$.

allows to conclude that there is a shift in metabolism towards oxidative phosphorylation [41] (Fig. 4, a and b, Table 2).

Glutamine deprivation differentially modulates lactate levels in the culture medium of U87MG and T98G cells. Significant increase in the lactate production was observed in the U87MG cells cultured in glutamine-free medium: calorimetrically assessed optical density was 1.99 ± 0.04 versus 1.42 ± 0.07 ($p < 0.01$). In contrast, for the T98G cells, decrease in the optical density of the solution was observed from 1.55 ± 0.05 to 0.96 ± 0.07, $p < 0.01$ (Fig. 4c). The obtained data confirm the changes observed by FLIM.

Glutamine deficiency modulates expression of the cytokine TRAIL signaling pathway components. It was shown in the recent work that glutamine deprivation in pancreatic cancer cells resulted in the decreased expression of antiapoptotic protein cFLIP, a caspase-8 homologue without protease activity, thereby increasing sensitivity of the cells to cytotoxic effects of the cytokine TRAIL; however, surface expression of the TRAIL target receptor DR5 was unchanged [42]. However, in our experiments with glioblastoma cells, the opposite effects were observed: upon glutamine deprivation, the cFLIP expression increased in the U87MG cells, but did not change in the T98G cells (Fig. 5a). In the U87MG cell, increase in the DR5 receptor expression was also observed both at the mRNA level, determined by RT-qPCR (Fig. 5b), and on the cell surface, as determined by flow cytometry (Fig. 5c), whereas the opposite trend was observed for the T98G cells (Fig. 5, b and c). This suggests that not only the cells of different tumor types, but also different cell lines of the same tumor type could respond differently to glutamine deprivation.

Glutamine deprivation in U87MG and T98G cells leads to opposite effects upon therapeutic treatments. Despite the proposed relationship between

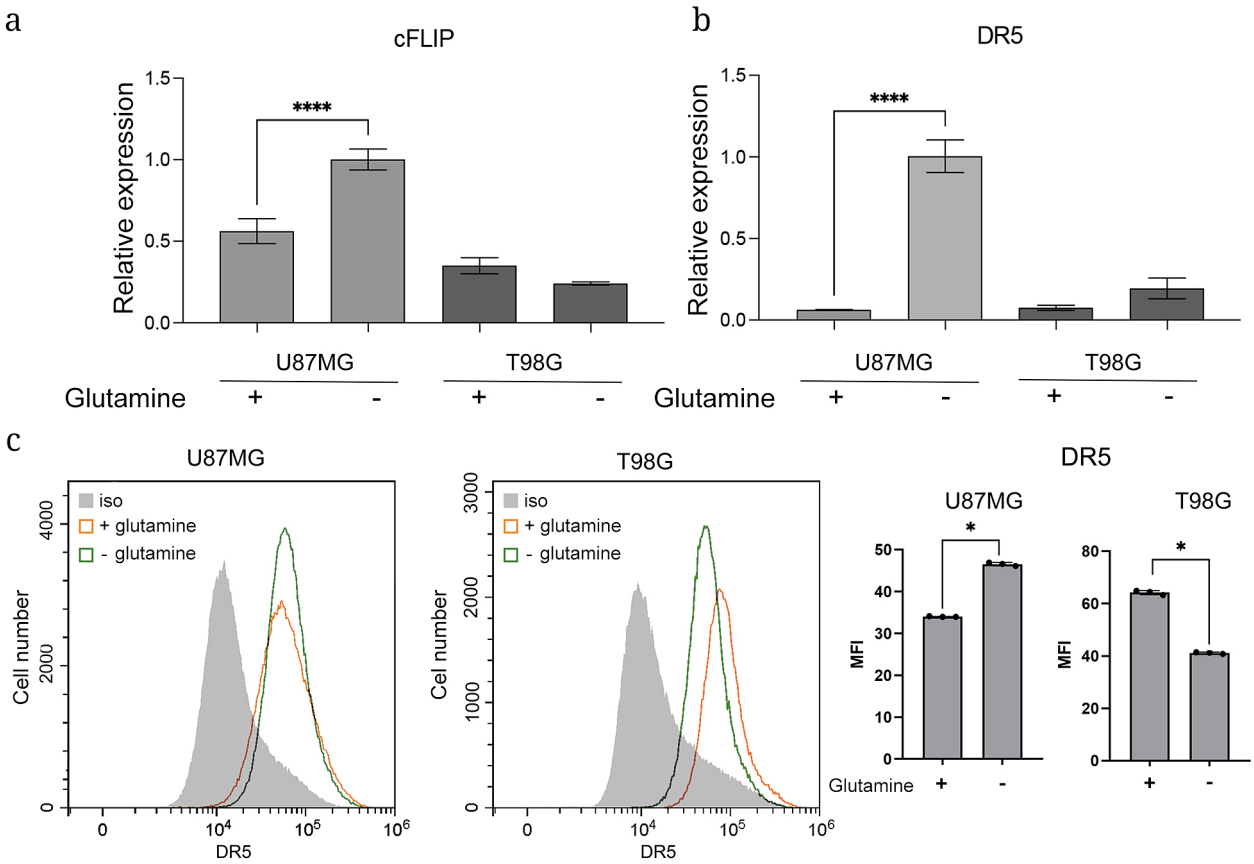

Fig. 5. DR5 and cFLIP expression in U87MG and T98G cell lines. Expression of (a) cFLIP and (b) DR5 at the mRNA level, **** $p < 0.005$. c) Expression of DR5 on the cell surface, * $p < 0.05$.

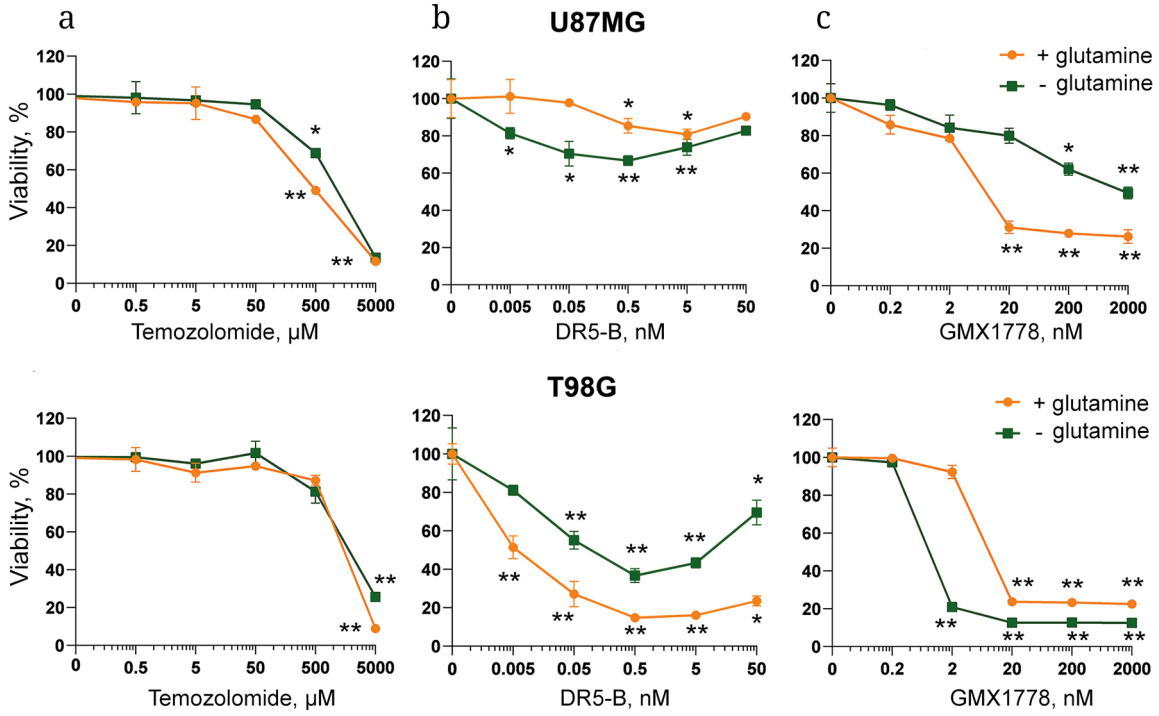

Fig. 6. Cytotoxicity of temozolomide (a), TRAIL DR5-B (b), and NAMPT inhibitor GMX1778 (c) for glioblastoma cell lines U87MG and T98G under standard conditions and upon glutamine deprivation, MTT test. * Significance compared to the control, $p < 0.05$; ** $p < 0.005$.

glutamine deprivation and tumor chemoresistance, glutamine deprivation did not affect sensitivity of both cell lines to temozolomide (Fig. 6a). However, cell sensitivity to the targeted DR5-specific cytokine TRAIL DR5-B differed significantly: glutamine deprivation sensitized the DR5-B-resistant U87MG cells, whereas the initially DR5-B-sensitive T98G cells, on the contrary, became more resistant to the DR5-mediated cell death (Fig. 6b). Such heterogeneous response of the U87MG and T98G cells to DR5-B correlates with the opposite changes in the expression of DR5 and cFLIP in these cells (Fig. 5). NAMPT inhibitor GMX1778 also induced opposite effects: in the absence of glutamine, resistance of the U87MG cells increased, while the T98G cells were sensitized to GMX1778 (Fig. 6c).

DISCUSSION

Metabolism of amino acids, particularly of glutamine, plays an important role in tumor development. In this regard, studying of the effects of glutamine deprivation on tumor cells is important both for identifying biochemical processes occurring in tumors and for the development of new potential therapies through the drug-induced deprivation of amino acids. In this work, we investigated the effect of glutamine deprivation on two human glioblastoma cell lines, U87MG and T98G, which differ in a number of characteristics. Transcriptome analysis revealed more differentiated phenotype of the U87MG cell line compared to the T98G cell line. Also, the data on differential activity of the genes associated with glutamine metabolism from the GSEA MSigDB Reactome Glutamate and Glutamine Metabolism database in U87MG cells relative to T98G (increased expression of GLUD1 and decreased expression of GOT2, PYCR3, PYCR1, GLUL, RIMKLA) pointed to possible differences in susceptibility of the cells to glutamine deprivation, as was observed in the subsequent experiments.

In particular, upon glutamine-free culturing, increased expression of the stem cell marker CD133 was observed in the U87MG cells, in contrast to the T98G cells. This could indicate de-differentiation of the U87MG cells, which is supported by a number of studies. For example, in the study by Pan et al., regional glutamine deficiency in the tumor core led to histone hypermethylation and caused de-differentiation of tumor cells [6]. In addition, de-differentiation of differentiated glioblastoma cells as a result of hypoxia in the tumor core was shown, which was accompanied by the increased expression of stemness markers and acidification of the core region [43, 44]. Overall, the process of de-differentiation of tumor cells under the influence of various triggers with activation of stemness genes and acquisition of properties similar to those of cancer stem cells has been described in the literature [45].

There are conflicting data regarding the effects of glutamine on tumor cell stemness. For example, glutamine deprivation or inhibition of glutaminase 1 (GLS1), which converts glutamine to glutamate, reduced expression of the stemness-related genes in hepatocellular carcinoma cells [46]. Similarly, glutamine deprivation inhibited tumor cell self-renewal and reduced expression of the stemness-related genes in the pancreatic cancer stem cells [47]. In contrast, in another study, glutamine deficiency in the ovarian and colon cancer cells caused metabolic reprogramming, leading to increased glycolysis, decreased proliferation, and increased population of tumor stem cells [48]. We observed similar conflicting effects in the U87MG and T98G cell lines.

Decrease in proliferation rate upon glutamine deprivation in our experiments was observed in both lines, but was more pronounced for the T98G cells than for the U87MG cells. Glioblastoma cell growth rate could be differentially affected by glutamine: lack of exogenous glutamine inhibits proliferation of the glioma cell lines D-54 MG, U-118 MG, and U-251 MG, but not U-373 MG, D-245 MG, and D-259 MG [36]. Later it was shown that the glioma stem cells are able to grow independently of exogenous glutamine, which is associated with the increased expression of glutamine synthetase (GLUL) [49]. However, recent work has shown that the tumors from the U87MG cell line, on the contrary, are glutamine dependent [50], correlating with the decreased level of GLUL expression and increased level of the GLUD1 expression (Fig. 2c), which also determines glutamine dependence [51]. This could be due to the absence of stem cell population, supporting our findings that the U87MG cells are highly differentiated. Unfortunately, the CD133 expression was not observed in the T98G cells, which, however, does not contradict their lower degree of differentiation, since the degree of stemness and differentiation is determined by the expression of various markers, among which CD133 is not the most specific [45].

It is known that inhibitors of the cyclin-dependent kinases $p21^{Waf1}$ and $p27^{KIP1}$ prevent proliferation and thereby maintain dormant state of stem cells and their ability to self-renew [52]. Therefore, increase in the $p21^{Waf1}$ and $p27^{KIP1}$ expression in U87MG cells along with the increase in CD133 correlates with the literature data reporting that activation of $p21^{Waf1}$ and $p27^{KIP1}$ maintained dormant state of the $CD133^{+}$ stem cells [53]. This also supports our hypothesis about de-differentiation of the U87MG cells upon glutamine deprivation. However, in the T98G cells, in contrast to the U87MG cells, increase in the expression of $p21^{Waf1}$ and $p27^{KIP1}$ was not statistically significant. This could be due to mutation in the p53 gene [54], since

proliferation of the T98G cells was inhibited through alternative mechanisms.

The differences revealed between the U87MG and T98G cell lines cultured in the absence of glutamine were accompanied by opposing metabolic processes. The NADH autofluorescence studies using FLIM-based metabolic imaging showed shift in the metabolic activity toward glycolysis in the U87MG cells, which was also confirmed by the increased lactate production. This correlates with the previously published data: for example, it was shown in the recent study that glutamine deprivation in the colorectal and pancreatic cancer cells leads to lysosomal acidification and induction of pro-survival autophagy. The study also demonstrated metabolic shift towards glycolysis under glutamine deprivation using the Seahorse™ glycolysis stress test and the CYRIS® flox multisensor cell analysis platform [37]. Increased glycolysis has also been shown as an adaptive response to glutamine deficiency in the glioblastoma cells [8]. Since the switch in metabolic activity towards oxidative phosphorylation has been previously shown during differentiation of stem [55, 56] and induced pluripotent cells [57, 58], the observed opposite shift towards glycolysis upon glutamine deprivation in the U87MG cells independently confirms the reverse process, i.e., de-differentiation of these cells.

Metabolic changes during glutamine deprivation in the T98G cells, unlike in the U87MG cells, were associated with the shift towards OXPHOS (oxidative phosphorylation), manifested both by NADH autofluorescence and by the decrease in lactate production. Previously, we and other researchers have shown that these changes correlate with the cell stress response. In particular, shift towards OXPHOS is a typical response to chemotherapy of various tumor cells including gliomas [59, 60]. Perhaps the opposite shifts towards glycolysis or OXPHOS observed upon glutamine deprivation in the U87MG and T98G lines, respectively, are due to metabolic plasticity of the tumor cells, which could determine sensitivity of the tumor cells to therapy. For example, high levels of OXPHOS were observed in the metformin-sensitive colorectal cancer line HT29, while the metformin-resistant SW620 cells had low levels of OXPHOS, but became sensitive to metformin upon glutamine deprivation [61]. Also, opposite effects of glutamine on sensitivity of the neuroblastoma cells to chemotherapy have been reported: glutamine deprivation suppressed the etoposide-induced apoptosis, but stimulated the cisplatin-induced apoptosis [62].

Based on this information, sensitivity of the U87MG and T98G cell lines to therapeutic effects of drugs of various nature was investigated in the next stage of our study: the conventional drug temozolomide, the DR5-specific cytokine TRAIL DR5-B, and the targeted inhibitor of nicotinamide phosphoribosyltransferase (NAMPT). Glutamine deprivation had no effect on sensitivity of either U87MG or T98G cells to temozolomide, but it significantly altered sensitivity of both cell lines to two other drugs. U87MG cells are initially resistant to the cytokine TRAIL DR5-B compared to the T98G cells, which correlates with their high degree of differentiation, since it is known that as the cells differentiate, surface expression of the TRAIL death receptors decreases [63, 64]. Consistent with this, glutamine deprivation in the U87MG cells resulted in the increased expression of DR5 and increased the DR5-mediated cell death, although the sensitizing effect was not pronounced, apparently due to increase in cFLIP, or due to mutation in the gene encoding PTEN phosphatase [54]. This correlates with the increased sensitivity of breast cancer [65] and pancreatic cancer cells to the TRAIL-mediated apoptosis upon glutamine deprivation [42]. Similarly, acute glutamine deprivation induced tumor cell apoptosis triggered by the CD95-mediated caspase cascade [66]. However, it should be noted that the T98G cell line, which was initially highly sensitive to the DR5-mediated cell death, on the contrary, became more resistant to DR5-B in the absence of glutamine, which was accompanied by the decrease in DR5 expression. Interestingly, similar results were previously obtained for the breast cancer

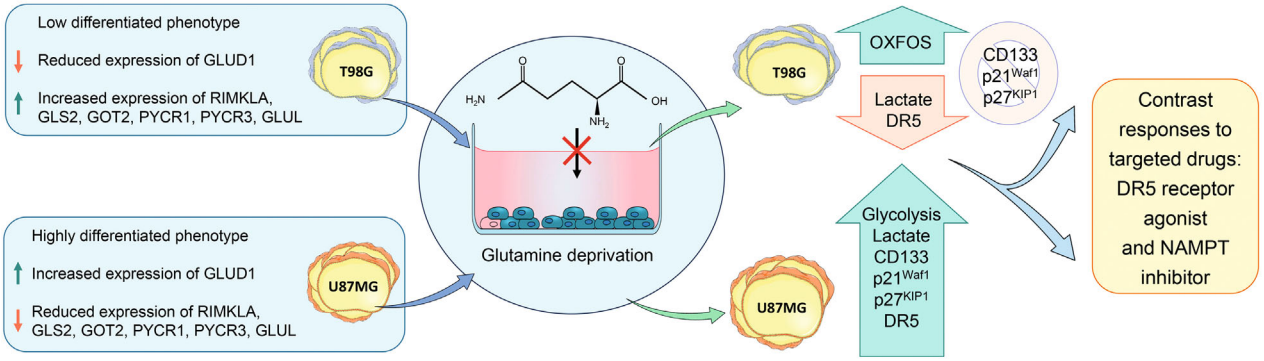

Fig. 7. Schematic representation of the opposite effects observed in the human glioblastoma cell lines U87MG and T98G upon glutamine deprivation.

cell lines: glutamine deprivation in the triple-negative breast cancer cells with basal (mesenchymal) phenotype increased their sensitivity to TRAIL, whereas the breast cancer cell lines with luminal phenotype were refractory to TRAIL sensitization upon glutamine deprivation [67]. Since the TRAIL signaling pathway plays an important role in the immunosurveillance of tumor cells, our findings support the known fact that glutamine metabolism could modulate antitumor immune response [68].

NAMPT is also a promising target in glioblastoma: in particular, its expression correlates with the degree of glioblastoma stemness and prognosis for patients [69]. Since glutamine is one of the sources of NAD(P)H [3], and NAMPT is the rate-limiting step in NAD biosynthesis, catalyzing formation of its intermediate product nicotinamide mononucleotide, these metabolic pathways are obviously interconnected. Recent data suggest that simultaneous drug-induced inhibition of glutaminolysis and NAD synthesis could become a successful strategy for cancer therapy [70]. As with the TRAIL DR5-B, contrasting effects were also observed in the U87MG and T98G cells when cultured in the absence of glutamine: the T98G cells were sensitized to the NAMPT inhibitor GMX1778, whereas the U87MG cells acquired resistance. This result correlates with the published data that the tumor cell resistance to NAMPT inhibitor is associated with the shift toward glycolysis [71], which we observed in the U87MG cells. Importantly, changes in the sensitivity of U87MG and T98G cells to GMX1778 upon glutamine deprivation were opposite to the changes in sensitivity to the DR5-mediated cell death, but mechanisms of this phenomenon remain to be elucidated.

Schematic representation of the effects observed in the U87MG and T98G cell lines upon glutamine deprivation are shown in Fig. 7.

CONCLUSION

Phenotypic and metabolic heterogeneity of human glioblastoma cells was demonstrated using two cell lines, U87MG and T98G. Upon glutamine deprivation, differences in the initial degree of differentiation and metabolic plasticity of these cell lines resulted in opposite metabolic changes and contrasting responses to the targeted drugs of various nature. Our data could potentially facilitate effective selection of the patients who could respond to the targeted therapy based on phenotypic and metabolic status of the tumor. In addition, the obtained results could help to identify mechanisms of tumor resistance associated with glutamine metabolism and facilitate development of the drug-induced glutamine deprivation regimens to enhance effectiveness of antitumor therapy.

Acknowledgments. The authors are grateful to D. N. Kazyulkin, A. V. Kurkin for providing GMX1778 and to V. V. Tatarskiy for providing primers, as well as to B. V. Chernyak and M. V. Shirmanova for valuable comments.

Contributions. A.V.Y. conceptualization, project administration, funding acquisition; A.A.I., D.V.M., K.S.K., I.N.D., and A.M.M. investigation, data curation, visualization; N.V.A., I.N.D., R.S.F., and M.E.G. methodology, validation; A.V.Y. and K.S.K. writing (original draft); I.N.D. and M.E.G. writing (review and editing).

Funding. The study was financially supported by the Russian Science Foundation, grant no. 24-24-00222, https://rscf.ru/project/24-24-00222/ (in Russian).

Ethics declarations. This work does not contain any studies involving human and animal subjects. The authors of this work declare that they have no conflicts of interest.

REFERENCES

1. Bergström, J., Fürst, P., Norée, L. O., and Vinnars, E. (1974) Intracellular free amino acid concentration in human muscle tissue, *J. Appl. Physiol.*, **36**, 693-697, https://doi.org/10.1152/jappl.1974.36.6.693.
2. Yang, L., Venneti, S., and Nagrath, D. (2017) Glutaminolysis: a hallmark of cancer metabolism, *Annu. Rev. Biomed. Engin.*, **19**, 163-194, https://doi.org/10.1146/annurev-bioeng-071516-044546.
3. DeBerardinis, R. J., Mancuso, A., Daikhin, E., Nissim, I., Yudkoff, M., Wehrli, S., and Thompson, C. B. (2007) Beyond aerobic glycolysis: Transformed cells can engage in glutamine metabolism that exceeds the requirement for protein and nucleotide synthesis, *Proc. Natl. Acad. Sci. USA*, **104**, 19345-19350, https://doi.org/10.1073/pnas.0709747104.
4. Shanware, N. P., Bray, K., Eng, C. H., Wang, F., Follettie, M., Myers, J., Fantin, V. R., and Abraham, R. T. (2014) Glutamine deprivation stimulates mTOR-JNK-dependent chemokine secretion, *Nat. Commun.*, **5**, 4900, https://doi.org/10.1038/ncomms5900.
5. Yuneva, M., Zamboni, N., Oefner, P., Sachidanandam, R., and Lazebnik, Y. (2007) Deficiency in glutamine but not glucose induces MYC-dependent apoptosis in human cells, *J. Cell Biol.*, **178**, 93-105, https://doi.org/10.1083/jcb.200703099.
6. Pan, M., Reid, M. A., Lowman, X. H., Kulkarni, R. P., Tran, T. Q., Liu, X., Yang, Y., Hernandez-Davies, J. E., Rosales, K. K., Li, H., Hugo, W., Song, C., Xu, X., Schones, D. E., Ann, D. K., Gradinaru, V., Lo, R. S., Locasale, J. W., and Kong, M. (2016) Regional glutamine deficiency in tumours promotes dedifferentiation through inhibition of histone demethylation, *Nat. Cell Biol.*, **18**, 1090-1101, https://doi.org/10.1038/ncb3410.

7. Márquez, J., Alonso, F. J., Matés, J. M., Segura, J. A., Martín-Rufián, M., and Campos-Sandoval, J. A. (2017) Glutamine addiction in gliomas, *Neurochem. Res.*, **42**, 1735-1746, https://doi.org/10.1007/s11064-017-2212-1.
8. Yin, H., Liu, Y., Dong, Q., Wang, H., Yan, Y., Wang, X., Wan, X., Yuan, G., and Pan, Y. (2024) The mechanism of extracellular CypB promotes glioblastoma adaptation to glutamine deprivation microenvironment, *Cancer Lett.*, **597**, 216862, https://doi.org/10.1016/j.canlet.2024.216862.
9. Jia, J. L., Alshamsan, B., and Ng, T. L. (2023) Temozolomide chronotherapy in glioma: a systematic review, *Curr. Oncol.*, **30**, 1893-1902, https://doi.org/10.3390/curroncol30020147.
10. Kuijlen, J. M., Mooij, J. J. A., Platteel, I., Hoving, E. W., Van Der Graaf, W. T. A., Span, M. M., Hollema, H., and den Dunnen, W. F. A. (2006) TRAIL-receptor expression is an independent prognostic factor for survival in patients with a primary glioblastoma multiforme, *J. Neuro Oncol.*, **78**, 161-171, https://doi.org/10.1007/s11060-005-9081-1.
11. Thang, M., Mellows, C., Mercer-Smith, A., Nguyen, P., and Hingtgen, S. (2023) Current approaches in enhancing TRAIL therapies in glioblastoma, *Neuro Oncol. Adv.*, **5**, vdad047, https://doi.org/10.1093/noajnl/vdad047.
12. Galli, U., Colombo, G., Travelli, C., Tron, G. C., Genazzani, A. A., and Grolla, A. A. (2020) Recent advances in NAMPT inhibitors: a novel immunotherapic strategy, *Front. Pharmacol.*, **11**, 656, https://doi.org/10.3389/fphar.2020.00656.
13. Fung, M. K. L., and Chan, G. C.-F. (2017) Drug-induced amino acid deprivation as strategy for cancer therapy, *J. Hematol. Oncol.*, **10**, 144, https://doi.org/10.1186/s13045-017-0509-9.
14. Jin, J., Byun, J.-K., Choi, Y.-K., and Park, K.-G. (2023) Targeting glutamine metabolism as a therapeutic strategy for cancer, *Exp. Mol. Med.*, **55**, 706-715, https://doi.org/10.1038/s12276-023-00971-9.
15. Jezierzański, M., Nafalska, N., Stopyra, M., Furgoł, T., Miciak, M., Kabut, J., and Gisterek-Grocholska, I. (2024) Temozolomide (TMZ) in the treatment of glioblastoma multiforme – a literature review and clinical outcomes, *Curr. Oncol.*, **31**, 3994-4002, https://doi.org/10.3390/curroncol31070296.
16. Gasparian, M. E., Chernyak, B. V., Dolgikh, D. A., Yagolovich, A. V., Popova, E. N., Sycheva, A. M., Moshkovskii, S. A., and Kirpichnikov, M. P. (2009) Generation of new TRAIL mutants DR5-A and DR5-B with improved selectivity to death receptor 5, *Apoptosis*, **14**, 778-787, https://doi.org/10.1007/s10495-009-0349-3.
17. Watson, M., Roulston, A., Bélec, L., Billot, X., Marcellus, R., Bédard, D., Bernier, C., Branchaud, S., Chan, H., Dairi, K., Gilbert, K., Goulet, D., Gratton, M.-O., Isakau, H., Jang, A., Khadir, A., Koch, E., Lavoie, M., Lawless, M., Nguyen, M., Paquette, D., Turcotte, É., Berger, A., Mitchell, M., Shore, G. C., and Beauparlant, P. (2009) The small molecule GMX1778 is a potent inhibitor of NAD $^+$ biosynthesis: strategy for enhanced therapy in nicotinic acid phosphoribosyltransferase 1-deficient tumors, *Mol. Cell. Biol.*, **29**, 5872-5888, https://doi.org/10.1128/MCB.00112-09.
18. Love, M. I., Huber, W., and Anders, S. (2014) Moderated estimation of fold change and dispersion for RNA-seq data with DESeq2, *Genome Biol.*, **15**, 550, https://doi.org/10.1186/s13059-014-0550-8.
19. Liberzon, A., Subramanian, A., Pinchback, R., Thorvaldsdóttir, H., Tamayo, P., and Mesirov, J. P. (2011) Molecular signatures database (MSigDB) 3.0, *Bioinformatics*, **27**, 1739-1740, https://doi.org/10.1093/bioinformatics/btr260.
20. Fang, Z., Liu, X., and Peltz, G. (2023) GSEApy: a comprehensive package for performing gene set enrichment analysis in Python, *Bioinformatics*, **39**, btac757, https://doi.org/10.1093/bioinformatics/btac757.
21. Ashburner, M., Ball, C. A., Blake, J. A., Botstein, D., Butler, H., Cherry, J. M., Davis, A. P., Dolinski, K., Dwight, S. S., Eppig, J. T., Harris, M. A., Hill, D. P., Issel-Tarver, L., Kasarskis, A., Lewis, S., Matese, J. C., Richardson, J. E., Ringwald, M., Rubin, G. M., and Sherlock, G. (2000) Gene Ontology: tool for the unification of biology, *Nat. Genet.*, **25**, 25-29, https://doi.org/10.1038/75556.
22. Kanehisa, M. (2000) KEGG: Kyoto encyclopedia of genes and genomes, *Nucleic Acids Res.*, **28**, 27-30, https://doi.org/10.1093/nar/28.1.27.
23. Gillespie, M., Jassal, B., Stephan, R., Milacic, M., Rothfels, K., Senff-Ribeiro, A., Griss, J., Sevilla, C., Matthews, L., Gong, C., Deng, C., Varusai, T., Ragueneau, E., Haider, Y., May, B., Shamovsky, V., Weiser, J., Brunson, T., Sanati, N., Beckman, L., Shao, X., Fabregat, A., Sidiropoulos, K., Murillo, J., Viteri, G., Cook, J., Shorser, S., Bader, G., Demir, E., Sander, C., Haw, R., Wu, G., Stein, L., Hermjakob, H., and D'Eustachio, P. (2022) The reactome pathway knowledgebase 2022, *Nucleic Acids Res.*, **50**, D687-D692, https://doi.org/10.1093/nar/gkab1028.
24. Martens, M., Ammar, A., Riutta, A., Waagmeester, A., Slenter, D. N., Hanspers, K., Miller, R. A., Digles, D., Lopes, E. N., Ehrhart, F., Dupuis, L. J., Winckers, L. A., Coort, S. L., Willighagen, E. L., Evelo, C. T., Pico, A. R., and Kutmon, M. (2021) WikiPathways: connecting communities, *Nucleic Acids Res.*, **49**, D613-D621, https://doi.org/10.1093/nar/gkaa1024.
25. Schaefer, C. F., Anthony, K., Krupa, S., Buchoff, J., Day, M., Hannay, T., and Buetow, K. H. (2009) PID: the pathway interaction database, *Nucleic Acids Res.*, **37**, D674-D679, https://doi.org/10.1093/nar/gkn653.
26. Xie, X., Lu, J., Kulbokas, E. J., Golub, T. R., Mootha, V., Lindblad-Toh, K., Lander, E. S., and Kellis, M. (2005) Systematic discovery of regulatory motifs in human promoters and 3′ UTRs by comparison of several

mammals, *Nature*, **434**, 338-345, https://doi.org/10.1038/nature03441.

27. Benjamini, Y., and Hochberg, Y. (1995) Controlling the false discovery rate: a practical and powerful approach to multiple testing, *J. R. Stat. Soc. Ser. B (Methodological)*, **57**, 289-300, https://doi.org/10.1111/j.2517-6161.1995.tb02031.x.
28. Yagolovich, A. V., Artykov, A. A., Dolgikh, D. A., Kirpichnikov, M. P., and Gasparian, M. E. (2019) A new efficient method for production of recombinant antitumor cytokine TRAIL and its receptor-selective variant DR5-B, *Biochemistry (Moscow)*, **84**, 627-636, https://doi.org/10.1134/S0006297919060051.
29. Suárez-Álvarez, B., Rodriguez, R. M., Calvanese, V., Blanco-Gelaz, M. A., Suhr, S. T., Ortega, F., Otero, J., Cibelli, J. B., Moore, H., Fraga, M. F., and López-Larrea, C. (2010) Epigenetic mechanisms regulate MHC and antigen processing molecules in human embryonic and induced pluripotent stem cells, *PLoS One*, **5**, e10192, https://doi.org/10.1371/journal.pone.0010192.
30. Vagaska, B., New, S. E. P., Alvarez-Gonzalez, C., D'Acquisto, F., Gomez, S. G., Bulstrode, N. W., Madrigal, A., and Ferretti, P. (2016) MHC-class-II are expressed in a subpopulation of human neural stem cells in vitro in an IFNγ-independent fashion and during development, *Sci. Rep.*, **6**, 24251, https://doi.org/10.1038/srep24251.
31. Liu, R., Zeng, L.-W., Li, H.-F., Shi, J.-G., Zhong, B., Shu, H.-B., and Li, S. (2023) PD-1 signaling negatively regulates the common cytokine receptor γ chain via MARCH5-mediated ubiquitination and degradation to suppress anti-tumor immunity, *Cell Res.*, **33**, 923-939, https://doi.org/10.1038/s41422-023-00890-4.
32. Yoo, H. C., Yu, Y. C., Sung, Y., and Han, J. M. (2020) Glutamine reliance in cell metabolism, *Exp. Mol. Med.*, **52**, 1496-1516, https://doi.org/10.1038/s12276-020-00504-8.
33. Yang, S., Hwang, S., Kim, M., Seo, S. B., Lee, J.-H., and Jeong, S. M. (2018) Mitochondrial glutamine metabolism via GOT2 supports pancreatic cancer growth through senescence inhibition, *Cell Death Dis.*, **9**, 55, https://doi.org/10.1038/s41419-017-0089-1.
34. Li, Y., Bie, J., Song, C., Liu, M., and Luo, J. (2021) PYCR, a key enzyme in proline metabolism, functions in tumorigenesis, *Amino Acids*, **53**, 1841-1850, https://doi.org/10.1007/s00726-021-03047-y.
35. Lodder-Gadaczek, J., Becker, I., Gieselmann, V., Wang-Eckhardt, L., and Eckhardt, M. (2011) N-acetylaspartylglutamate synthetase II synthesizes N-acetylaspartylglutamylglutamate, *J. Biol. Chem.*, **286**, 16693-16706, https://doi.org/10.1074/jbc.M111.230136.
36. Dranoff, G., Elion, G. B., Friedman, H. S., Campbell, G. L., and Bigner, D. D. (1985) Influence of glutamine on the growth of human glioma and medulloblastoma in culture, *Cancer Res.*, **45**, 4077-4081.
37. Lengauer, F., Geisslinger, F., Gabriel, A., von Schwarzenberg, K., Vollmar, A. M., and Bartel, K. (2023) A metabolic shift toward glycolysis enables cancer cells to maintain survival upon concomitant glutamine deprivation and V-ATPase inhibition, *Front. Nutr.*, **10**, 1124678, https://doi.org/10.3389/fnut.2023.1124678.
38. Blacker, T. S., and Duchen, M. R. (2016) Investigating mitochondrial redox state using NADH and NADPH autofluorescence, *Free Radic. Biol. Med.*, **100**, 53-65, https://doi.org/10.1016/j.freeradbiomed.2016.08.010.
39. Kolenc, O. I., and Quinn, K. P. (2019) Evaluating cell metabolism through autofluorescence imaging of NAD(P)H and FAD, *Antioxid. Redox Signal.*, **30**, 875-889, https://doi.org/10.1089/ars.2017.7451.
40. Skala, M. C., Riching, K. M., Bird, D. K., Gendron-Fitzpatrick, A., Eickhoff, J., Eliceiri, K. W., Keely, P. J., and Ramanujam, N. (2007) In vivo multiphoton fluorescence lifetime imaging of protein-bound and free nicotinamide adenine dinucleotide in normal and precancerous epithelia, *J. Biomed. Optics*, **12**, 024014, https://doi.org/10.1117/1.2717503.
41. Song, A., Zhao, N., Hilpert, D. C., Perry, C., Baur, J. A., Wallace, D. C., and Schaefer, P. M. (2024) Visualizing subcellular changes in the NAD(H) pool size versus redox state using fluorescence lifetime imaging microscopy of NADH, *Commun. Biol.*, **7**, 428, https://doi.org/10.1038/s42003-024-06123-7.
42. Kim, J. H., Lee, J., Im, S. S., Kim, B., Kim, E.-Y., Min, H.-J., Heo, J., Chang, E.-J., Choi, K.-C., Shin, D.-M., and Son, J. (2024) Glutamine-mediated epigenetic regulation of cFLIP underlies resistance to TRAIL in pancreatic cancer, *Exp. Mol. Med.*, **56**, 1013-1026, https://doi.org/10.1038/s12276-024-01231-0.
43. Li, P., Zhou, C., Xu, L., and Xiao, H. (2013) Hypoxia enhances stemness of cancer stem cells in glioblastoma: an *in vitro* study, *Int. J. Med. Sci.*, **10**, 399-407, https://doi.org/10.7150/ijms.5407.
44. Larionova, T. D., Bastola, S., Aksinina, T. E., Anufrieva, K. S., Wang, J., Shender, V. O., Andreev, D. E., Kovalenko, T. F., Arapidi, G. P., Shnaider, P. V., Kazakova, A. N., Latyshev, Y. A., Tatarskiy, V. V., Shtil, A. A., Moreau, P., Giraud, F., Li, C., Wang, Y., Rubtsova, M. P., Dontsova, O. A., Condro, M., Ellingson, B. M., Shakhparonov, M. I., Kornblum, H. I., Nakano, I., and Pavlyukov, M. S. (2022) Alternative RNA splicing modulates ribosomal composition and determines the spatial phenotype of glioblastoma cells, *Nat. Cell Biol.*, **24**, 1541-1557, https://doi.org/10.1038/s41556-022-00994-w.
45. Najafi, M., Farhood, B., and Mortezaee, K. (2019) Cancer stem cells (CSCs) in cancer progression and therapy, *J. Cell. Physiol.*, **234**, 8381-8395, https://doi.org/10.1002/jcp.27740.
46. Li, B., Cao, Y., Meng, G., Qian, L., Xu, T., Yan, C., Luo, O., Wang, S., Wei, J., Ding, Y., and Yu, D. (2019) Targeting glutaminase 1 attenuates stemness properties in hepatocellular carcinoma by increasing reactive oxygen species and suppressing Wnt/beta-catenin pathway,

EBioMedicine, **39**, 239-254, https://doi.org/10.1016/j.ebiom.2018.11.063.

47. Li, D., Fu, Z., Chen, R., Zhao, X., Zhou, Y., Zeng, B., Yu, M., Zhou, Q., Lin, Q., Gao, W., Ye, H., Zhou, J., Li, Z., Liu, Y., and Chen, R. (2015) Inhibition of glutamine metabolism counteracts pancreatic cancer stem cell features and sensitizes cells to radiotherapy, *Oncotarget*, **6**, 31151-31163, https://doi.org/10.18632/oncotarget.5150.
48. Prasad, P., Ghosh, S., and Roy, S. S. (2021) Glutamine deficiency promotes stemness and chemoresistance in tumor cells through DRP1-induced mitochondrial fragmentation, *Cell. Mol. Life Sci.*, **78**, 4821-4845, https://doi.org/10.1007/s00018-021-03818-6.
49. Tardito, S., Oudin, A., Ahmed, S. U., Fack, F., Keunen, O., Zheng, L., Miletic, H., Sakariassen, P. Ø., Weinstock, A., Wagner, A., Lindsay, S. L., Hock, A. K., Barnett, S. C., Ruppin, E., Mørkve, S. H., Lund-Johansen, M., Chalmers, A. J., Bjerkvig, R., Niclou, S. P., and Gottlieb, E. (2015) Glutamine synthetase activity fuels nucleotide biosynthesis and supports growth of glutamine-restricted glioblastoma, *Nat. Cell Biol.*, **17**, 1556-1568, https://doi.org/10.1038/ncb3272.
50. Wang, L., Han, Y., Gu, Z., Han, M., Hu, C., and Li, Z. (2023) Boosting the therapy of glutamine-addiction glioblastoma by combining glutamine metabolism therapy with photo-enhanced chemodynamic therapy, *Biomater. Sci.*, **11**, 6252-6266, https://doi.org/10.1039/D3BM00897E.
51. Wang, Q., Wu, M., Li, H., Rao, X., Ao, L., Wang, H., Yao, L., Wang, X., Hong, X., Wang, J., Aa, J., Sun, M., Wang, G., Liu, J., and Zhou, F. (2022) Therapeutic targeting of glutamate dehydrogenase 1 that links metabolic reprogramming and Snail-mediated epithelial-mesenchymal transition in drug-resistant lung cancer, *Pharmacol. Res.*, **185**, 106490, https://doi.org/10.1016/j.phrs.2022.106490.
52. Ezoe, S., Matsumura, I., Satoh, Y., Tanaka, H., and Kanakura, Y. (2004) Cell cycle regulation in hematopoietic stem/progenitor cells, *Cell Cycle (Georgetown, Tex.)*, **3**, 314-318.
53. Wei, Y., Chen, Q., Huang, S., Liu, Y., Li, Y., Xing, Y., Shi, D., Xu, W., Liu, W., Ji, Z., Wu, B., Chen, X., and Jiang, J. (2022) The interaction between DNMT1 and high-mannose CD133 maintains the slow-cycling state and tumorigenic potential of glioma stem cell, *Adv. Sci.*, **9**, 2202216, https://doi.org/10.1002/advs.202202216.
54. Ishii, N., Maier, D., Merlo, A., Tada, M., Sawamura, Y., Diserens, A.-C., and van Meir, E. G. (1999) Frequent co-alterations of *TP53*, *p16/CDKN2A*, *p14* ^{ARF}, *PTEN* tumor suppressor genes in human glioma cell lines, *Brain Pathol.*, **9**, 469-479, https://doi.org/10.1111/j.1750-3639.1999.tb00536.x.
55. Wanet, A., Arnould, T., Najimi, M., and Renard, P. (2015) Connecting mitochondria, metabolism, and stem cell fate, *Stem Cells Dev.*, **24**, 1957-1971, https://doi.org/10.1089/scd.2015.0117.
56. Pattappa, G., Heywood, H. K., De Bruijn, J. D., and Lee, D. A. (2011) The metabolism of human mesenchymal stem cells during proliferation and differentiation, *J. Cell. Physiol.*, **226**, 2562-2570, https://doi.org/10.1002/jcp.22605.
57. Rodimova, S. A., Meleshina, A. V., Kalabusheva, E. P., Dashinimaev, E. B., Reunov, D. G., Torgomyan, H. G., Vorotelyak, E. A., and Zagaynova, E. V. (2019) Metabolic activity and intracellular pH in induced pluripotent stem cells differentiating in dermal and epidermal directions, *Methods Appl. Fluores.*, **7**, 044002, https://doi.org/10.1088/2050-6120/ab3b3d.
58. Rodimova, S., Mozherov, A., Elagin, V., Karabut, M., Shchechkin, I., Kozlov, D., Krylov, D., Gavrina, A., Kaplin, V., Epifanov, E., Minaev, N., Bardakova, K., Solovieva, A., Timashev, P., Zagaynova, E., and Kuznetsova, D. (2023) FLIM imaging revealed spontaneous osteogenic differentiation of stem cells on gradient pore size tissue-engineered constructs, *Stem Cell Res. Ther.*, **14**, 81, https://doi.org/10.1186/s13287-023-03307-6.
59. Morelli, M., Lessi, F., Barachini, S., Liotti, R., Montemurro, N., Perrini, P., Santonocito, O. S., Gambacciani, C., Snuderl, M., Pieri, F., Aquila, F., Farnesi, A., Naccarato, A. G., iacava, P., Cardarelli, F., Ferri, G., Mulholland, P., Ottaviani, D., Paiar, F., Liberti, G., Pasqualetti, F., Menicagli, M., Aretini, P., Signore, G., Franceschi, S., and Mazzanti, C. M. (2022) Metabolic-imaging of human glioblastoma live tumors: a new precision-medicine approach to predict tumor treatment response early, *Front. Oncol.*, **12**, 969812, https://doi.org/10.3389/fonc.2022.969812.
60. Yuzhakova, D. V., Sachkova, D. A., Shirmanova, M. V., Mozherov, A. M., Izosimova, A. V., Zolotova, A. S., and Yashin, K. S. (2023) Measurement of patient-derived glioblastoma cell response to temozolomide using fluorescence lifetime imaging of NAD(P)H, *Pharmaceuticals*, **16**, 796, https://doi.org/10.3390/ph16060796.
61. Kim, J. H., Lee, K. J., Seo, Y., Kwon, J.-H., Yoon, J. P., Kang, J. Y., Lee, H. J., Park, S. J., Hong, S. P., Cheon, J. H., Kim, W. H., and Il Kim, T. (2018) Effects of metformin on colorectal cancer stem cells depend on alterations in glutamine metabolism, *Sci. Rep.*, **8**, 409, https://doi.org/10.1038/s41598-017-18762-4.
62. Valter, K., Chen, L., Kruspig, B., Maximchik, P., Cui, H., Zhivotovsky, B., and Gogvadze, V. (2017) Contrasting effects of glutamine deprivation on apoptosis induced by conventionally used anticancer drugs, *Biochim. Biophys. Acta Mol. Cell Res.*, **1864**, 498-506, https://doi.org/10.1016/j.bbamcr.2016.12.016.
63. Siegmund, D., Lang, I., and Wajant, H. (2017) Cell death-independent activities of the death receptors CD 95, TRAILR 1, and TRAILR 2, *FEBS J.*, **284**, 1131-1159, https://doi.org/10.1111/febs.13968.

64. Galluzzi, L., Vitale, I., Aaronson, S. A., Abrams, J. M., Adam, D., Agostinis, P., Alnemri, E. S., Altucci, L., Amelio, I., Andrews, D. W., Annicchiarico-Petruzzelli, M., Antonov, A. V., Arama, E., Baehrecke, E. H., Barlev, N. A., Bazan, N. G., Bernassola, F., Bertrand, M. J. M., Bianchi, K., Blagosklonny, M. V., Blomgren, K., Borner, C., Boya, P., Brenner, C., Campanella, M., Candi, E., Carmona-Gutierrez, D., Cecconi, F., Chan, F. K.-M., Chandel, N. S., Cheng, E. H., Chipuk, J. E., Cidlowski, J. A., Ciechanover, A., Cohen, G. M., Conrad, M., et al. (2018) Molecular mechanisms of cell death: recommendations of the Nomenclature Committee on Cell Death 2018, *Cell Death Differ.*, **25**, 486-541, https://doi.org/10.1038/s41418-017-0012-4.
65. Dilshara, M. G., Jeong, J.-W., Prasad Tharanga Jayasooriya, R. G., Neelaka Molagoda, I. M., Lee, S., Park, S. R., Choi, Y. H., and Kim, G.-Y. (2017) Glutamine deprivation sensitizes human breast cancer MDA-MB-231 cells to TRIAL-mediated apoptosis, *Biochem. Biophys. Res. Commun.*, **485**, 440-445, https://doi.org/10.1016/j.bbrc.2017.02.059.
66. Fumarola, C., Zerbini, A., and Guidotti, G. G. (2001) Glutamine deprivation-mediated cell shrinkage induces ligand-independent CD95 receptor signaling and apoptosis, *Cell Death Differ.*, **8**, 1004-1013, https://doi.org/10.1038/sj.cdd.4400902.
67. Mauro-Lizcano, M., and López-Rivas, A. (2018) Glutamine metabolism regulates FLIP expression and sensitivity to TRAIL in triple-negative breast cancer cells, *Cell Death Dis.*, **9**, 205, https://doi.org/10.1038/s41419-018-0263-0.
68. Wang, B., Pei, J., Xu, S., Liu, J., and Yu, J. (2024) A glutamine tug-of-war between cancer and immune cells: recent advances in unraveling the ongoing battle, *J. Exp. Clin. Cancer Res.*, **43**, 74, https://doi.org/10.1186/s13046-024-02994-0.
69. Lucena-Cacace, A., Otero-Albiol, D., Jiménez-García, M. P., Peinado-Serrano, J., and Carnero, A. (2017) NAMPT overexpression induces cancer stemness and defines a novel tumor signature for glioma prognosis, *Oncotarget*, **8**, 99514-99530, https://doi.org/10.18632/oncotarget.20577.
70. Hasan Bou Issa, L., Fléchon, L., Laine, W., Ouelkdite, A., Gaggero, S., Cozzani, A., Tilmont, R., Chauvet, P., Gower, N., Sklavenitis-Pistofidis, R., Brinster, C., Thuru, X., Touil, Y., Quesnel, B., Mitra, S., Ghobrial, I. M., Kluza, J., and Manier, S. (2024) MYC dependency in GLS1 and NAMPT is a therapeutic vulnerability in multiple myeloma, *iScience*, **27**, 109417, https://doi.org/10.1016/j.isci.2024.109417.
71. Thongon, N., Zucal, C., D'Agostino, V. G., Tebaldi, T., Ravera, S., Zamporlini, F., Piacente, F., Moschoi, R., Raffaelli, N., Quattrone, A., Nencioni, A., Peyron, J.-F., and Provenzani, A. (2018) Cancer cell metabolic plasticity allows resistance to NAMPT inhibition but invariably induces dependence on LDHA, *Cancer Metab.*, **6**, 1, https://doi.org/10.1186/s40170-018-0174-7.